

文章编号: 1000-324X(2023)02-0125-12

DOI: 10.15541/jim20220338

冷烧结技术的研究现状及发展趋势

冯静静¹, 章游然^{1,2}, 马名生¹, 陆毅青¹, 刘志甫^{1,2}

(1. 中国科学院 上海硅酸盐研究所, 中科院无机功能材料与器件重点实验室, 上海 201899; 2. 中国科学院大学 材料科学与光电技术学院, 北京 100049)

摘要: 采用常规热烧结实现陶瓷粉体的致密化, 烧结温度通常超过 1000 °C, 这不仅需要消耗大量能源, 还会使一些陶瓷材料在物相稳定性、晶界控制以及与金属电极共烧等方面面临挑战。近年来提出的冷烧结技术(Cold Sintering Process, CSP)可将烧结温度降低至 400 °C 以下, 利用液相形式的瞬态溶剂和单轴压力, 通过陶瓷颗粒的溶解-沉淀过程实现陶瓷材料的快速致密化。冷烧结技术具有烧结温度低和时间短等特点, 自开发以来受到广泛关注, 目前已应用于近百种陶瓷及陶瓷基复合材料, 涉及电介质材料、半导体材料、压敏材料和固态电解质材料等。本文介绍了冷烧结技术的发展历程、工艺技术及其致密化机理, 对其在陶瓷材料及陶瓷-聚合物复合材料领域的研究现状进行了综述, 其中根据溶解性的差异主要介绍了 Li₂MoO₄ 陶瓷、ZnO 陶瓷和 BaTiO₃ 陶瓷的冷烧结现状。针对冷烧结技术工艺压力高的问题及可能的解决途径进行了探讨, 并对冷烧结技术未来的发展趋势进行了展望。

关键词: 冷烧结技术; 陶瓷; 复合材料; 溶剂; 综述

中图分类号: TQ174 文献标志码: A

Current Status and Development Trend of Cold Sintering Process

FENG Jingjing¹, ZHANG Youran^{1,2}, MA Mingsheng¹, LU Yiqing¹, LIU Zhifu^{1,2}

(1. Key Laboratory of Inorganic Functional Materials and Devices, Shanghai Institute of Ceramics, Chinese Academy of Sciences, Shanghai 201899, China; 2. College of Materials Science and Opto-Electronic Technology, University of Chinese Academy of Sciences, Beijing 100049, China)

Abstract: Densification of ceramic materials by conventional sintering process usually requires a high temperature over 1000 °C, which not only consumes a lot of energy, but also forces some ceramic materials to face challenges in phase stability, grain boundary control, and co-firing with metal electrodes. In recent years, an extremely low temperature sintering technique named cold sintering process (CSP) was proposed, which can reduce the sintering temperature to below 400 °C, and realize the rapid densification of ceramic materials through the dissolution-precipitation process of ceramic particles by using the transient solvent in liquid phase and uniaxial pressure. The advantages of CSP, including low sintering temperature and short sintering time, have attracted extensive attention from researchers, since it was firstly reported in 2016. At present, CSP has been applied to the sintering of nearly 100 kinds of ceramics and ceramic-matrix composites, involving dielectric materials, semiconductor materials, pressure-sensitive materials, and solid-state electrolyte materials. This paper firstly introduces the low-temperature

收稿日期: 2022-06-17; 收到修改稿日期: 2022-07-29; 网络出版日期: 2022-09-15

基金项目: 中国博士后科学基金(2021M693264); 国家自然科学基金(61871369)

China Postdoctoral Science Foundation (2021M693264); National Natural Science Foundation of China (61871369)

作者简介: 冯静静(1989-), 女, 博士. E-mail: fengjingjing@mail.sic.ac.cn

FENG Jingjing (1989-), female, PhD. E-mail: fengjingjing@mail.sic.ac.cn

通信作者: 刘志甫, 研究员. E-mail: liuzf@mail.sic.ac.cn

LIU Zhifu, professor. E-mail: liuzf@mail.sic.ac.cn

sintering techniques' development history, process and densification mechanism. Then, application of CSP in the field of ceramic materials and ceramic-polymer composites is summarized. Based on differences of solubility, application of CSP mainly on Li_2MoO_4 ceramics, ZnO ceramics, BaTiO_3 ceramics, and their composites preparations are introduced. Auxiliary effect of the transient solvent on cold sintering process is emphatically analyzed. Moreover, the high pressure issue in the cold sintering process and the possible solutions are discussed. At last, future development trend of cold sintering process is prospected.

Key words: cold sintering process; ceramic; composite; solvent; review

陶瓷烧结是通过物质迁移，使陶瓷粉体固结成致密块体的过程，其历史最早可追溯至旧石器时代晚期(公元前 25000 年)，时至今日陶瓷的烧结仍受到全世界的广泛关注^[1-3]。实际烧结过程一般需要施加外界作用来影响烧结热力学和/或动力学因素，进一步驱动传质过程。早期的常规烧结以加热作为外界作用，主要通过增大原子迁移率影响烧结动力学，进而促进烧结过程中的传质。但由于大多数无机材料的熔点较高，而常规烧结通常在原料粉体熔点的 50%~75% 温度范围内完成，因此烧结温度一般超过 1000 °C，且烧结时间长达数小时甚至数天^[4]。这样的高温过程必然消耗大量能源，对实验装置的要求也极高，而且高温还会加速陶瓷粉体中挥发性元素(如铋、铅、钠、钾等)损失，造成不可控的晶界缺陷问题。此外，不同材料共烧时，高温也会使产物出现非预期的化学反应、分层、开裂等问题^[5-8]。

自 20 世纪以来，开发低温烧结技术一直备受全球学者关注^[9-10]。与常规烧结将温度作为唯一的传质驱动力不同，低温烧结技术引入电场、溶剂、压力等外场来改变烧结热力学和动力学条件。其中，电场主要通过增强加热效应、增大原子迁移率影响烧结动力学因素^[11-12]；溶剂主要通过液相扩散和塑性变形影响烧结动力学；外施的压力则为烧结过程提供了额外的驱动力，影响烧结热力学因素。根据所施加外界作用(温度、电场、溶剂、压力)的不同，可将目前的烧结技术归纳为图 1，其中不同烧结技术的缩写及定义列于表 1^[13-14]。

由此可见，低温烧结技术创新的关键在于结合不同的外场作用共同驱动材料的致密化，已广泛应用的低温烧结技术主要有闪烧(Flash Sintering, FS)^[15-16]、冷烧结技术(Cold Sintering Technology, CSP)^[17-21]、放电等离子体烧结(Spark Plasma Sintering, SPS)^[22-23]、水热热压烧结(Hydrothermal Hot Press Sintering, HHP)^[24-28]等。其中，冷烧结技术以操作方便、设备简单、烧结温度较低等优势受到广泛关注。本文介绍了冷烧结技术的发展历程、工艺技术及其烧结机

制，对冷烧结技术在陶瓷材料以及陶瓷-聚合物复合材料领域的研究现状进行了总结。并针对冷烧结技术工艺压力高的问题及可能的解决途径进行了探讨，对冷烧结技术未来的发展趋势进行了展望。

1 冷烧结技术概述

1.1 发展历程

1986 年，日本高知大学的 Yamasaki 团队^[25]首次将水热法与单轴压力相结合应用于陶瓷的低温烧结，在 350 °C 下成功获得致密陶瓷烧结体，并将该技术定义为水热热压烧结(HHP)。由于设备复杂、产品尺寸形状受限、所得试样致密度较低等因素，水热热压烧结并未得到深入的研究。近年来，研究者们在水热热压烧结的基础上，对设备简单、适用范围广的低温烧结技术进行了持续的研究和探索^[8,29]。

2016 年，美国宾夕法尼亚州立大学的 Randall 团队^[17-21]在水热热压烧结的基础上提出了一种新型超低温烧结技术，并命名为冷烧结技术(CSP)。该团队利用水溶液形式的瞬态溶剂(水、醋酸溶液、碱溶液等)，在 100~500 MPa 的单轴压力和较短的时间内，实现了 NaCl 、 Li_2MoO_4 、 V_2O_5 和 BaTiO_3 等多种陶瓷材料的低温烧结(室温至 300 °C)，所得产品的致

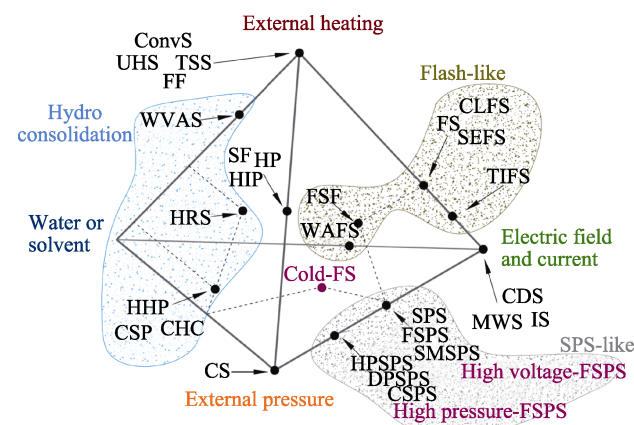


图 1 烧结技术四元图^[13]

Fig. 1 Quaternary diagram of sintering techniques^[13]

表 1 烧结技术定义表^[13-14]
Table 1 Definition table of sintering techniques^[13-14]

Technique	Name (Abbreviation)	Definition
Traditional sintering	Conventional sintering (ConvS)	Thermal sintering at heating rate of 1–10 °C/min
	Two step sintering (TSS)	Thermal sintering divided in two steps (heating; cooling and densification)
	Fast firing (FF)	Rapid sintering with short soaking times and high heating rates
	Sinter forging (SF)	Sintering in presence of uniaxial pressure in die-less configuration
	Hot pressing (HP)	Sintering at high temperature and in presence of uniaxial pressure
Liquid phase sintering	Hydrothermal hot pressing (HIP)	Sintering at high temperature and in presence of hydrostatic pressure
	Cold sintering process (CSP)	Sintering at $T < 400$ °C in presence of solvent and uniaxial pressure
	Cold hydrostatic consolidation (CHC)	Sintering at room temperature in presence of solvent and hydrostatic pressure
	Hydrothermal hot pressing (HHP)	Pressure-assisted sintering in hydrothermal conditions
	Hydrothermal reaction sintering (HRS)	Sintering of oxide ceramics in presence of supercritical water
	Water vapor-assisted sintering (WVAS)	Conventional sintering in a humid atmosphere
Flash-like	Reactive hydrothermal liquid-phase densification (rHLPD)	Sintering at low temperature assisted by hydrothermal reaction
	Flash sintering (FS)	Rapid sintering at low furnace temperature in presence of electric field
	Thermally insulated flash sintering (TIFS)	Flash sintering where the sample is thermally insulated from the environment
	Flash sinterforging (FSF)	Flash sintering in presence of uniaxial pressure in die-less configuration
	Sliding electrodes flash sintering (SEFS)	Flash sintering where the electrodes are in relative motion with respect to the sample
	Water-assisted flash sintering (WAFS)	Flash sintering in humid atmosphere
SPS-like	Contactless flash sintering (CLFS)	Flash sintering with electrodes in non-contact mode
	Spark plasma sintering (SPS)	Sintering in presence of a DC electric potential and uniaxial pressure
	Deformable punch spark plasma sintering (DPSPS)	Spark plasma sintering at very high pressure (1000–2000 MPa)
	Flash spark plasma sintering (FSPS)	Hybrid technique of flash sintering and spark plasma sintering
	Cool spark plasma sintering (CSPS)	Spark plasma sintering at $T < 400$ °C and high pressure (300–600 MPa)
	High pressure spark plasma sintering (HPSPS)	Spark plasma sintering at high pressure (10^2 – 10^3 MPa)
Others	Sacrificial material spark plasma sintering (SMPS)	Spark plasma sintering with a sacrificial die to form samples with complex shapes
	Ultrafast high-temperature sintering (UHS)	Rapid sintering at heating rate of 10^3 – 10^4 °C/min
	Cold sintering (CS)	Sintering of ductile materials at high pressure and low temperature
	Microwave sintering (MWS)	Densification assisted by heating with an electromagnetic radiation
	Induction sintering (IS)	Densification assisted by heating with an induction system
	Capacitor discharge sintering (CDS)	Rapid sintering with electric energy supplied by capacitor discharge

密度可达 90%以上。随后, 来自欧洲和亚洲的研究团队也陆续采用该方法成功实现了 CaCO_3 ^[30]、 $\text{Al}_2\text{SiO}_5\text{-NaCl}$ ^[31]、 $\text{Al}_2\text{O}_3\text{-NaCl}$ ^[32]、 $\text{Na}_{0.5}\text{Bi}_{0.5}\text{MoO}_4\text{-Li}_2\text{MoO}_4$ ^[33]等 70 余种陶瓷材料的低温致密化。可见, 冷烧结技术为陶瓷的低温烧结提供了适用性较广的新思路^[34]。

1.2 冷烧结工艺

目前尚未定义 CSP 的标准化工艺和装置, 从已有报道来看, 所有材料冷烧结都涉及溶剂引入、单轴压力加压、加热等几个要素, 主要过程如下: 首先, 将适量的溶剂加入陶瓷粉体中, 使颗粒表

面均匀润湿, 以促进液相与固相之间的紧密接触; 然后, 将润湿的陶瓷原料倒入室温或经预热后的模具中, 通过液压机或机械压力机施加单轴压力; 当压力达到最大负载时, 通过模具上方和下方的热压板或包裹在模具周围的电控加热套加热(<400 °C), 得到结构较致密的陶瓷烧结体。有研究报道的冷烧结陶瓷晶粒发育不完善, 晶界处存在非晶相, 还会对样品进行后处理来进一步提高致密度, 从而获得最佳结构与性能^[17,35-36]。CSP 所用装置为开放式体系, 允许溶剂通过模具间隙蒸发, 与其他需要专用密封反应釜(如 HHP)或昂贵电极(如 FS)的低温烧结技术相比设备需

求简单,使CSP成为一种更方便易行的烧结技术^[4,37]。

1.3 冷烧结致密化机理

由于CSP概念提出时间较短,对其烧结机理的理解还不成熟。目前,研究者们普遍认为冷烧结过程可分为两个阶段,如图2所示^[20,38]。第一阶段是在室温下的加压过程,主要发生陶瓷颗粒的局部溶解、重排和压实。在该过程中,陶瓷粉体在中间液相作用下均匀润湿,颗粒表面形成一层液膜。这层液膜会引起颗粒尖端的局部溶解,并作为润滑剂加速颗粒的重排和滑移。此时适当的压力作用有利于颗粒重排和填充孔隙,从而进一步提高压实过程中的颗粒堆积密度^[20]。

第二阶段是在恒定压力下加热至最高温度并保温的过程,这是陶瓷粉体致密化的关键阶段,研究认为该阶段的致密化机制主要有溶解-沉淀和塑性变形两种。对于水溶性较好的陶瓷粉体,主要进行陶瓷颗粒溶解、沉淀以及晶粒生长。在该过程中,颗粒溶解由溶剂与陶瓷粉体之间的动态化学作用驱动,可通过多种方式实现,包括螯合、脱水和团簇反应^[39]。随着恒定压力下温度升高,中间液相持续蒸发的同时,溶液逐渐达到过饱和状态,从而使溶解的陶瓷粉体以沉淀的形式析出。另外,由于孔隙区域的化学势低于颗粒接触区域,溶解的原子团簇或离子会迁移至化学势较低的孔隙位置并沉淀,从而降低表面能并逐步实现陶瓷材料的致密化。其中,由化学势梯度驱动的沉淀过程可以认为等同于地质学中岩层形成的压力-溶解蠕变过程^[40-41]。该阶段溶解-沉淀过程中析出的沉淀物可以是结晶相或非晶相,晶粒周围包覆的非晶相会限制晶粒进一步生长。因此,在一定的工艺条件下,CSP可以烧结制备亚微米陶瓷或纳米陶瓷^[7]。

除了上述溶解-沉淀机制,通过黏性流动或位

错运动的塑性变形也是冷烧结的致密化机制之一,可以很好地解释微溶或难溶材料通过冷烧结技术的致密化过程^[40-43]。例如,Bouville等^[30]以水为溶剂,在室温下冷烧结纳米球霰石陶瓷材料,虽然该陶瓷粉体在水中的溶解性较差,但产物的相对密度可达82%。同样,BaTiO₃虽然难溶于水,但以水为溶剂,通过冷烧结得到的陶瓷材料的相对密度可达90%以上^[44]。这些材料的致密化显然不能通过溶解-沉淀机制来解释,此时塑性变形可能是其冷烧结过程中的主要致密化机制。

2 冷烧结技术在材料烧结中的应用

2.1 陶瓷材料

冷烧结技术已被广泛应用于氯化物、氧化物、磷酸盐等70余种陶瓷材料(表2)的烧结,涉及微波电介质^[31-33,45-46]、固态电解质^[47]和半导体材料^[48-49]等。采用冷烧结技术制备的大部分陶瓷材料具有较高的致密度,并且可以达到与传统高温烧结技术相媲美的性能。CSP极低的烧结温度还为探索高温易分解的亚稳态陶瓷材料提供了新思路。本文以目前研究最为广泛的Li₂MoO₄、ZnO和BaTiO₃三种陶瓷材料体系为例,介绍冷烧结在陶瓷材料制备领域的研究现状。

2.1.1 Li₂MoO₄陶瓷

碱金属钼酸盐(Li₂MoO₄、Na₂Mo₂O₇和K₂Mo₂O₇等)不仅具有较低的熔点(<1000 °C),而且具有较高的水溶解度,这些特点有助于其在冷烧结过程中更充分地进行溶解-沉淀,实现低温下的充分致密化。碱金属钼酸盐是应用冷烧结技术制备最早的材料体系,并且获得了良好的微波介电性能。下面仅以Li₂MoO₄为例,介绍其在冷烧结技术中的研究现状。

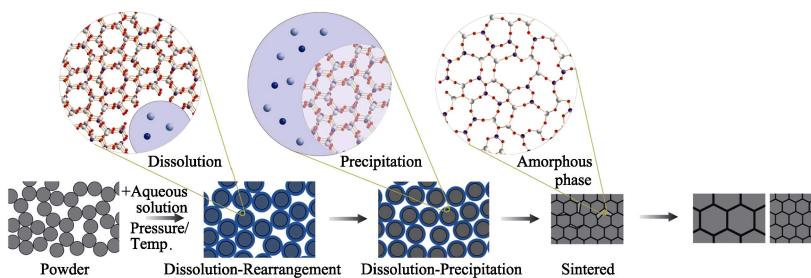


图2 冷烧结的致密化机理示意图^[20,38]
Fig. 2 Schematic diagram of densification mechanism of CSP^[20,38]

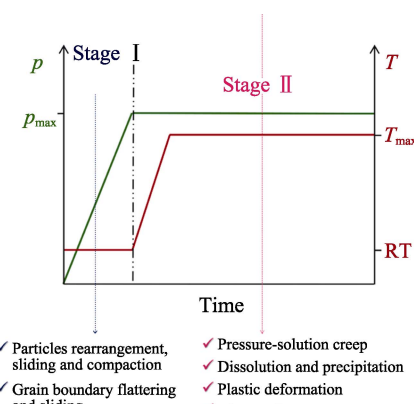


表 2 通过冷烧结技术制备的陶瓷材料^[29,38,50]
Table 2 Ceramic materials prepared by CSP^[29,38,50]

Binary compound	Ternary compound	Quaternary compound	Quinary compound
MoO ₃	Li ₂ CO ₃	LiFePO ₄	LiAl _{0.5} Ge _{1.5} (PO ₄) ₃
WO ₃	CsSO ₄	LiCoPO ₄	Li _{0.5x} Bi _{1-0.5x} Mo _x V _{1-x} O ₄
V ₂ O ₃	Li ₂ MoO ₄	KH ₂ PO ₄	(Bi _{0.95} Li _{0.05})(V _{0.9} Mo _{0.1})O ₄
V ₂ O ₅	Na ₂ Mo ₂ O ₇	Ca ₅ (PO ₄) ₃ (OH)	Li _{1.5} Al _{0.5} Ge _{1.5} (PO ₄) ₃
ZnO	K ₂ Mo ₂ O ₇	(LiBi) _{0.5} MoO ₄	—
Bi ₂ O ₃	ZnMoO ₄	CsH ₂ PO ₄	—
Fe ₂ O ₃	K ₂ MoO ₄	InGaZnO ₄	—
SiO ₂	Bi ₂ Mo ₂ O ₉	K _{0.5} Na _{0.5} NbO ₃	—
CsBr	Gd ₂ (MoO ₄) ₃	LiFePO ₄	—
MgO	Li ₂ WO ₄	Li ₂ Mg ₃ TiO ₆	—
PbTe	Na ₂ WO ₄	Na _{0.5} Bi _{0.5} MoO ₄	—
Bi ₂ Te ₃	LiVO ₃	Na _{0.5} Bi _{0.5} TiO ₃	—
NaCl	BiVO ₄	YBa ₂ Cu ₃ O _{7-x}	—
ZnTe	AgVO ₃	—	—
AgI	Na ₂ ZrO ₃	—	—
CuCl	BaTiO ₃	—	—
ZrF ₄	NaNO ₂	—	—
ZrO ₂	Mg ₂ P ₂ O ₇	—	—
Al ₂ O ₃	BaMoO ₄	—	—
CeO ₂	Cs ₂ WO ₄	—	—
MnO	Na _x CO ₂ O ₄	—	—
SnO	Ca ₃ Co ₄ O ₉	—	—
TiO ₂	KPO ₃	—	—
MoS ₂	Al ₂ SiO ₅	—	—
—	Ca ₃ Co ₄ O ₉	—	—
—	CaCO ₃	—	—
—	BaFe ₁₂ O ₁₉	—	—
—	ZrW ₂ O ₈	—	—
—	NaNbO ₃	—	—
—	SrTiO ₃	—	—

早在 2014 年, Kahari 等^[51]就在室温条件下成功制备出致密度较高的 Li₂MoO₄ 陶瓷, 他们以少量水为液相均匀润湿 Li₂MoO₄ 粉末, 同时施加 130 MPa 的单轴压力, 在室温和 120 °C 下分别保温 4 h 进行恒温恒压致密化。所制得的试样均为纯 Li₂MoO₄ 相, 致密度为 87%~93%, 可与 540 °C 常规高温烧结相媲美。此外, 不同温度下低温致密化所制得试样的相对介电常数 ϵ_r 均为 4.6~5.2, 但由于室温下存在残余水, 室温固结样品的品质因数 $Q \times f$ 值低于 120 °C 低温烧结样品。此阶段, Li₂MoO₄ 冷烧结陶瓷的致密度和微波介电性能还有待进一步优化。

2016 年, Guo 等^[20]以去离子水为中间液相, 在 120 °C 和 100~500 MPa 单轴压力下对 Li₂MoO₄ 粉体进行 15~20 min 的保温, 成功制备出无杂相、致密

度>90%的 Li₂MoO₄ 冷烧结微波介质陶瓷, 其微波介电性能可与 540 °C 传统高温烧结相媲美。在 120 °C 和 350 MPa 单轴压力下保温 15 min, Li₂MoO₄ 冷烧结陶瓷的致密度可达 95.7%, 相对介电常数 ϵ_r 为 5.6, 品质因数 $Q \times f$ 为 30500 GHz, 温度系数 TCF 为 $-1.74 \times 10^{-4} \text{ }^{\circ}\text{C}^{-1}$ 。他们还发现在该条件下冷烧结的陶瓷晶粒与原始粉体颗粒的尺寸相近(图 3)。因此, Guo 等^[20]指出 CSP 可以用于烧结制备亚微米级或纳米级晶粒尺寸的新型功能陶瓷材料。此研究充分证明了 CSP 的可行性及其技术优势, 故 Li₂MoO₄ 等钼酸盐体系的微波介质陶瓷自研发以来一直是冷烧结陶瓷的代表性范例。

2.1.2 ZnO 陶瓷

ZnO 由于地球资源丰富、价格低廉、表面化学可调控、电学性能优良等优势, 在半导体、电化学和催化等领域有着广泛的应用, 越来越受到材料科学界的关注与重视。但传统热烧结制备的 ZnO 陶瓷的晶粒过度生长, 存在结构缺陷, 相应的性能有所降低。纳米 ZnO 粉体具有丰富的晶粒形态、良好的溶剂亲和性、较高的表面活性和一致的溶解性, 是一种比较适合通过 CSP 制备的陶瓷材料^[52]。

然而, ZnO 在水中的溶解性较差, 以水作为溶剂进行冷烧结很难达到较高的致密度, 相应的性能也会有所恶化。针对这一问题, 研究者发现可以通过调整溶剂的 pH 来改善陶瓷颗粒在溶剂中的溶解性, 或者在冷烧结液相中引入适宜浓度的陶瓷原料阳离子, 进一步驱动陶瓷材料的烧结致密化^[53]。Funahashi 等^[54]分别以水和不同浓度的乙酸溶液作为中间液相, 对难溶于水的 ZnO 粉体进行冷烧结, 发现以水为溶剂的冷烧结 ZnO 陶瓷样品显微结构中存在大量孔隙, 且相对密度仅为 65% 左右。而随着冷烧结液相中乙酸的加入, ZnO 陶瓷样品的晶粒尺寸明显增大, 当乙酸溶液浓度增加至 1 mol/L 时, 样品的致密度可达 98%, 显微结构如图 4 所示^[54]。在单轴压力 77 MPa 和 305 °C 的条件下保温 2 h 制备的 ZnO 陶瓷样品电导率为 9 S/cm, 高于传统

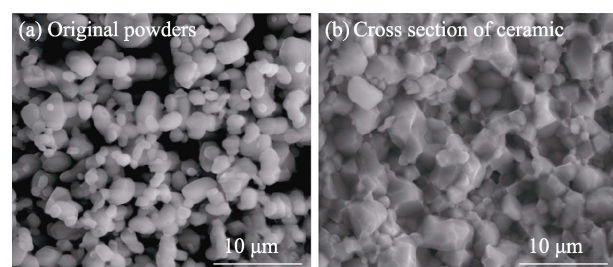


图 3 冷烧结前后 Li₂MoO₄ 的 SEM 照片^[20]

Fig. 3 SEM images of Li₂MoO₄ before and after cold sintering^[20]
(a) Original powders; (b) Cross section of ceramics

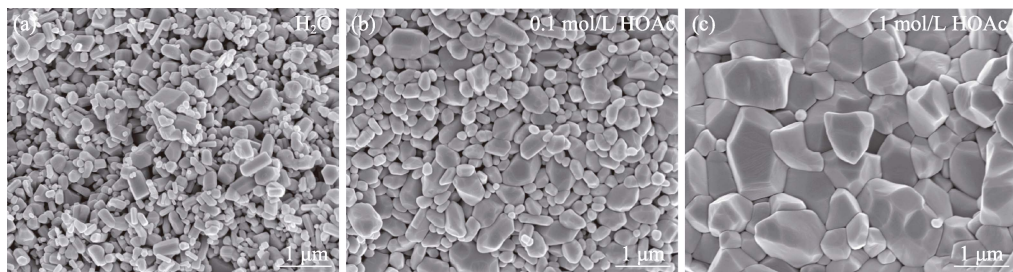


图4 以不同溶剂冷烧结制备ZnO陶瓷的SEM照片^[54]
Fig. 4 SEM images of cold sintered ZnO ceramics with different solvents^[54]
(a) Water; (b) 0.1 mol/L acetic acid; (c) 1 mol/L acetic acid

1400 °C高温烧结ZnO样品(5 S/cm),表明引入低沸点乙酸并未恶化ZnO陶瓷的电学性能。Kang等^[55]对ZnO陶瓷冷烧结液相中离子种类、浓度和pH的影响进行了研究,发现虽然液相的pH能影响陶瓷粉体的溶解性,但它与ZnO陶瓷样品致密度的关联性并不大。同样是在单轴压力530 MPa和120 °C下保温0.5 h,以pH 7的水为溶剂得到的ZnO陶瓷样品相对密度仅为71%,但以pH 7的0.83 mol/L乙酸锌溶液为溶剂得到的ZnO陶瓷样品相对密度可达99%,这表明液相中足量的CH₃COO⁻和Zn²⁺是实现ZnO陶瓷致密化的关键。其中,CH₃COO⁻可以通过降低液相pH,提高ZnO颗粒的溶解性;Zn²⁺则通过增大液相与固体颗粒之间的化学势梯度,加速冷烧结的传质过程。二者的协同作用实现了ZnO陶瓷的高度致密化。

2.1.3 BaTiO₃陶瓷

BaTiO₃因其高介电常数和低介电损耗等特性,在电介质陶瓷材料领域占有举足轻重的地位,是电子陶瓷领域内应用最广泛的材料之一。因此,BaTiO₃陶瓷冷烧结技术的研究在材料科学领域备受关注。但是BaTiO₃不仅在水中溶解度有限,而且Ba²⁺和Ti⁴⁺的溶解速率也不一致,其中Ba²⁺优先溶解于水中,产生无定形的TiO₂包覆在粉体颗粒周围,形成“惰性表面”,使水溶液与固相粉体分隔开,阻碍溶解-沉淀过程,故而以水作为溶剂很难实现BaTiO₃陶瓷的冷烧结^[53]。

2016年,Guo等^[17,35]采用Ba(OH)₂、TiO₂与水

混合而成的悬浮液作为中间液相,180 °C保温0.5 h制备了冷烧结BaTiO₃陶瓷。其中悬浮液中的Ba²⁺和Ti⁴⁺均处于饱和状态,从而有效抑制BaTiO₃颗粒的不一致溶解。但由于制得的样品中BaTiO₃晶体周围被大量BaCO₃非晶相包覆,介电性能较差,后续需进行900 °C热处理消除杂相,使非晶相结晶,才能改善样品的介电性能。为解决这一问题,2020年,Tsuji等^[56]以熔融的NaOH-KOH混合碱溶液作为液相助烧剂,在单轴压力520 MPa和300 °C的条件下保温12 h,便可一步制得高度致密化的纳米BaTiO₃陶瓷,并且无需后续热处理。其显微结构如图5(a, b)所示,可以发现样品无明显的孔隙和非晶相,致密度可达98%~99%,晶粒尺寸为75~150 nm。由试样的介电温谱图(图5(c))可知,冷烧结BaTiO₃陶瓷具有与常规热烧结相当的优良介电性能,在1 MHz下测得的室温相对介电常数ε_r为700~1800,介电损耗约为0.04。但该方法的工艺条件较为苛刻,使BaTiO₃陶瓷-聚合物复合材料的制备受限,其中聚合物难以承受高温高压的强碱环境。因此,近期Sada等^[57]引入Ba(OH)₂·8H₂O作为液相助烧剂对BaTiO₃进行冷烧结,该方法无需后续热处理并且工艺条件较温和。在单轴压力350 MPa、烧结温度低至150 °C的条件下保温15 h使BaTiO₃一步致密化,得到的BaTiO₃陶瓷致密度可达95%,在1 MHz下的室温相对介电常数超过1000,其显微结构和介电温谱图如图6所示。

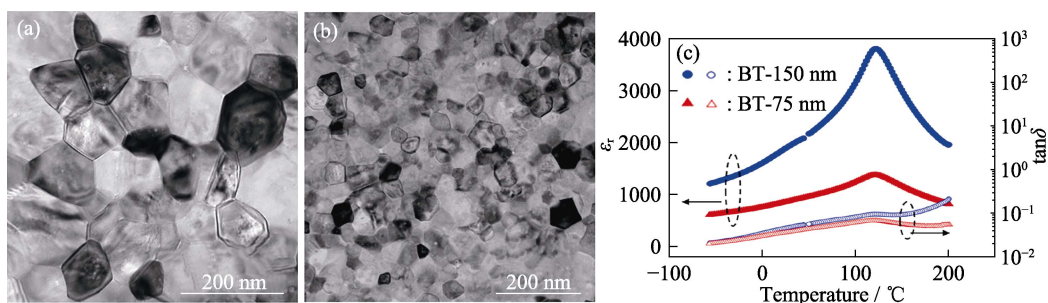
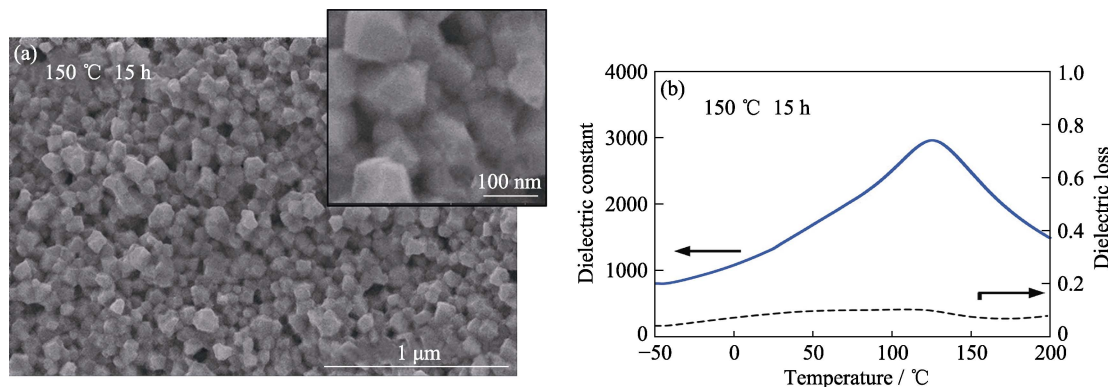


图5 300 °C 保温 12 h 冷烧结的 BaTiO₃ 陶瓷^[56]
Fig. 5 Cold sintered BaTiO₃ ceramics obtained by holding at 300 °C for 12 h^[56]
TEM images with grain size of 150 nm (a) and 75 nm (b); (c) Dielectric temperature spectra at 1 MHz

图 6 150 °C 下保温 15 h 冷烧结的 BaTiO₃ 陶瓷^[57]Fig. 6 Cold sintered BaTiO₃ ceramics obtained by holding at 150 °C for 15 h^[57]
(a) SEM images; (b) Dielectric temperature spectra at 1 MHz

2.2 陶瓷-聚合物复合材料

许多无机材料常规热烧结的烧结温度超过 1000 °C, 而高分子材料在此高温下易分解, 导致陶瓷和聚合物材料的共烧之间存在天然的鸿沟, 如图 7(a)所示。冷烧结技术的烧结温度低, 使加工温度窗口大相径庭的陶瓷和聚合物材料共同烧结成为可能。目前已通过冷烧结技术成功制备了近 20 种陶瓷-聚合物复合材料(如表 3 所示), 可应用于电介质、半导体、压敏电阻和固态电解质等众多领域^[38]。聚合物填料以热塑性聚合物最为常见, 体积含量约 2%~30% 最为适宜, 一般均匀分散在陶瓷晶界位置或层压在陶瓷层片之间(如图 7(b)所示), 在不阻碍陶瓷致密化的同时起到改善材料性能的作用。

2016 年, Guo 等^[19]通过冷烧结技术成功制备了三种性能各异的复合材料, 分别为 (1-x)Li₂MoO₄-xPTFE(聚四氟乙烯)微波电介质材料、(1-x)Li_{1.5}Al_{0.5}Ge_{1.5}(PO₄)₃(LAGP)/xPVDF-HFP(聚偏氟乙烯-六氟丙烯共聚物)固态电解质材料、(1-x)V₂O₅-xPEDOT:PSS(聚(3,4-乙撑二氧噻吩)-聚苯乙烯磺酸)半导体材料, 三者的性能与聚合物含量的关系如图 8 所示。其中, (1-x)Li₂MoO₄-xPTFE (x=0~70%, 体积分数)冷烧结复合材料的相对介电常数

ϵ_r 符合对数混合定律, 约为 2.9~5.8, 品质因数 $Q \times f$ 值在 17700~25200 GHz 范围内没有发生恶化的现象, 温度系数 TCF 随 x 的增大而大幅提升, 表明加入 PTFE 使材料的温度稳定性得到改善。其次, 该团队将(1-x)LAGP/xPVDF-HFP($x=0\sim40\%$, 体积分数)冷烧结试样浸泡吸收 5%~10% 的 LiPF₆/EC-DMC(六氟磷酸锂/碳酸乙烯酯-二甲基碳酸酯)电解液, 使试样中形成快速离子运输通道, 室温离子电导率由 6.1×10^{-7} S/cm 大幅提升至 1.0×10^{-4} S/cm。在(1-x)V₂O₅-xPEDOT:PSS($x=0\sim30\%$, 体积分数)冷烧结复合材料中, 由于 PEDOT:PSS 属于导电聚合物, 其 1%~2% 的添加量即可将 V₂O₅ 的室温电导率提升 1~2 个数量级, 电导活化能下降至 0.22 eV。

2018 年, Zhao 等^[62]以乙酸溶液为液相, 通过冷烧结技术成功制备了高致密度的(1-x)ZnO-xPTFE($x=0\sim40\%$, 体积分数)复合材料。其中 PTFE 添加量为 5%(体积分数)时的显微结构如图 9(a, b)所示, 可以发现 PTFE 绝缘材料均匀分布于半导电的 ZnO 陶瓷晶粒的晶界位置, 厚度为 1~10 nm。这种界面结构形成了高阻的肖特基势垒, 如图 9(c)所示, 阻碍电子的跃迁, 从而使 ZnO-PTFE 复合材料呈现出非线性的压敏特性, 其非线性系数 α 为 7.03。随着 PTFE 添加

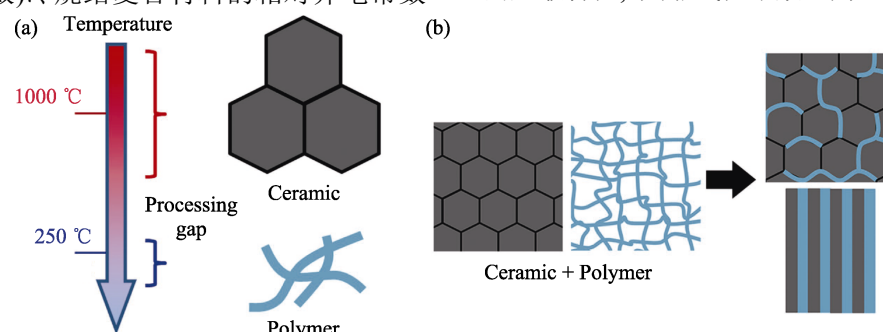
图 7 陶瓷-聚合物复合材料示意图^[34]Fig. 7 Schematic diagrams of ceramic-polymer composites^[34]
(a) Processing temperature gap; (b) Composite formed by CSP

表3 通过冷烧结技术制备的复合材料
Table 3 Composites prepared by CSP

Ceramic-polymer composite	Solvent	Processing conditions	Relative density	Application	Ref.
Li_2MoO_4 -PTFE	Deionized (DI) water	120 °C, 350 MPa, 15–20 min	96%–97%	Dielectrics	[19]
$\text{Li}_{1.5}\text{Al}_{0.5}\text{Ge}_{1.5}(\text{PO}_4)_3$ /PVDF-HFP	DI water	120 °C, 400 MPa, 60 min	80%–86%	Li-ion battery electrolytes	[19]
V_2O_5 -PEDOT:PSS	DI water	120 °C, 350 MPa, 20–30 min	91%–93%	Negative-temperature-resistance sensors	[19,58]
$(\text{LiBi})_{0.5}\text{MoO}_4$ -PTFE	DI water	120 °C, 250–350 MPa, 20 min	>85%	Dielectrics	[21]
$\text{Na}_2\text{Mo}_2\text{O}_7$ -PEI	DI water	120 °C, 175–350 MPa, 20 min	>90%	Dielectrics	[59]
SiO_2 -PTFE	TEOS/NaOH	270 °C, 430 MPa, 60 min	90%–99%	Dielectrics	[60]
BaTiO_3 -PTFE	$\text{Ba}(\text{OH})_2 \cdot 8\text{H}_2\text{O}$	225 °C, 350 MPa, 120 min	>90%	Dielectrics	[61]
ZnO-PTFE	Acetic acid	300 °C, 350 MPa, 30 min	93%–99%	Varistors	[62]
LiFePO ₄ -C-PVDF	LiOH	240 °C, 30–750 MPa, 30 min	89%	Li-ion electrodes	[63]
NaNbO_3 -PVDF	DI water	180 °C, 550 MPa, 10 min	97%	Dielectrics	[64]
ZnO-PEEK	Acetic acid	330 °C, 300 MPa, 120 min	>98%	Varistors	[65-66]
ZnO-PDMS	Acetic acid	250 °C, 320 MPa, 60 min	>90%	Varistors	[67]
ZnO/PVDF-TrFE	Acetic acid	140 °C, 300 MPa, 240 min	>95%	Varistors	[68]
ZnO-PEI-Mn ₂ O ₃ -CoO	Acetic acid	150 °C, 27 MPa, 60 min	88%	Varistors	[69]
LiFePO_4 - $\text{Li}_{6.95}\text{Mg}_{0.15}\text{La}_{2.75}\text{Sr}_{0.25}$	DMF	100–140°C, 400 MPa, 90–180 min	>85%	Li-ion battery electrolytes	[70]
Zr_2O_{12} -PPC-LiClO ₄					

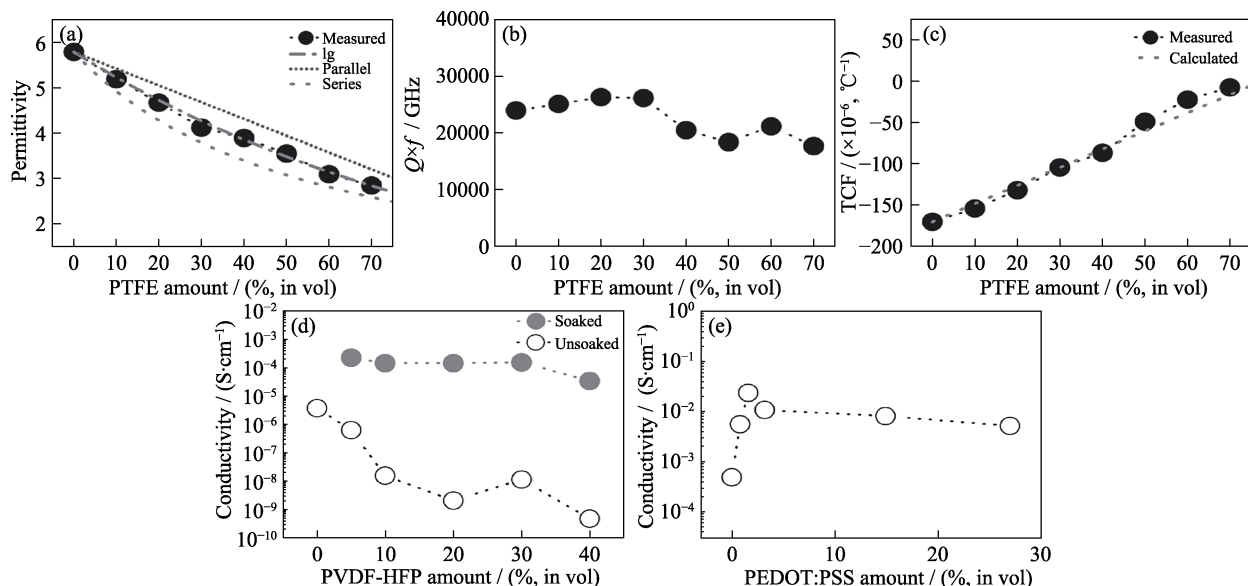


图8 三种冷烧结复合材料的电性能^[19]

Fig. 8 Electrical properties of three composites prepared by cold sintering process^[19]

(a-c) ϵ_r , $Q \times f$, TCF of $(1-x)\text{Li}_2\text{MoO}_4$ -xPTFE; (d) Conductivity of $(1-x)\text{LAGP}/x\text{PVDF-HFP}$; (e) Conductivity of $(1-x)\text{V}_2\text{O}_5$ -xPEDOT:PSS

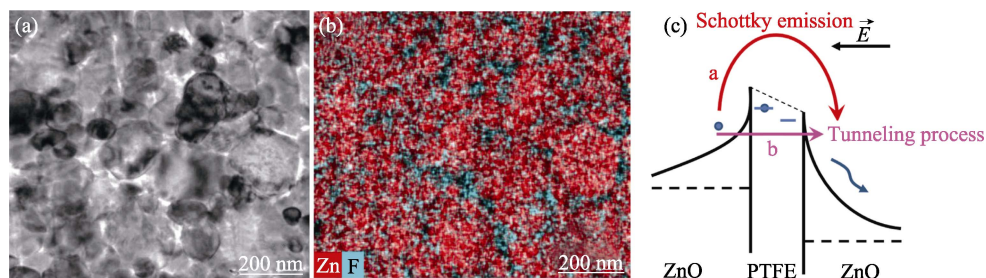


图9 冷烧结ZnO-PTFE复合材料^[62]

Fig. 9 Cold sintered ZnO-PTFE composites^[62]

(a) TEM image; (b) EDS image; (c) Schematic diagram of Schottky barrier structure

量的增大, 复合材料的晶界活化能从 0.2 eV 提高至 0.76 eV。此外, Beauvoir 等^[71]还发现加入 PTFE 使冷烧结过程中溶剂的自由流动受限, 导致 ZnO 陶瓷晶粒沿垂直于外施单轴压力的方向取向生长。

2021 年, Sada 等^[57]以 $\text{Ba}(\text{OH})_2 \cdot 8\text{H}_2\text{O}$ 为液相助烧剂, 实现了 BaTiO_3 与体积分数 5% PTFE 的冷烧结共烧, 其显微结构与性能如图 10 所示。 BaTiO_3 -PTFE 冷烧结复合材料总体上具有均匀且致密的微观结构, 但部分区域内存在 PTFE 偏析。在性能方面, 该复合材料的电阻率与纯 BaTiO_3 冷烧结陶瓷相比提高了 4 个数量级, 高达 $10^{12} \Omega \cdot \text{m}$ 。此外, 该复合材料还具有较高的室温相对介电常数, 在 1 MHz 下达到 790, 同时介电损耗仅为 0.014, 低于纯 BaTiO_3 冷烧结陶瓷的损耗(0.09)。以上研究工作充分证明, 通过冷烧结制备陶瓷-聚合物复合材料的可行性和设计多样性, 冷烧结技术不仅弥合了陶瓷与聚合物材料的加工温度差, 而且实现了陶瓷-聚合物复合材料性能的可调控化, 展现出广阔的应用前景。

3 冷烧结技术的发展趋势

冷烧结技术以其烧结温度低、时间短等优势, 自开发以来受到广泛关注, 可应用的材料体系层出不穷, 但目前仍处于实验室研究阶段, 尚未投入工

业化的大规模生产。其中最关键的制约因素是冷烧结技术需要施加较高的单轴压力, 一般为 350~500 MPa, 这不但对工艺设备的要求极高, 而且仅可制备形状简单的小尺寸试样。

为了解决这一问题, Bang 等^[69]通过增大试样尺寸至表面积为 25 cm^2 , 在单轴压力 27 MPa、烧结温度 140 °C 的工艺条件下, 分别实现了 ZnO 和 LAGP 陶瓷的冷烧结, 致密度可达 90% 以上, 如图 11 所示, 证实了降低单轴压力实现冷烧结致密化的可行性。但增大试样尺寸也带来了新的问题, 烧结过程中瞬态液相溶剂的不均匀挥发, 导致冷烧结试样各区域的结构不均一。其中 ZnO 陶瓷呈现出明显的半透明区和不透明区, 两区域的材料具有完全不一致的晶体结构、厚度和硬度(图 12), 而 LAGP 陶瓷则在高度结晶相之间存在一定的非晶相。

除了增大试样尺寸外, 目前低温低压烧结的另一研究方向是借助化学作用降低烧结势垒, 从而实现材料的致密化。2016 年, 美国新泽西州立罗格斯大学的 Riman 团队^[72]在水热热压烧结的基础上开发了反应水热液相致密化(rHLPD)技术。该技术是一种不同于冷烧结技术的低温致密化技术, 涉及水热反应、渗透、反应结晶和液相烧结机理, 利用该技术制备 $\text{BaTiO}_3/\text{TiO}_2$ 陶瓷的致密化过程如图 13 所示。首先通过常规的造粒和排胶工序制备 TiO_2 多孔

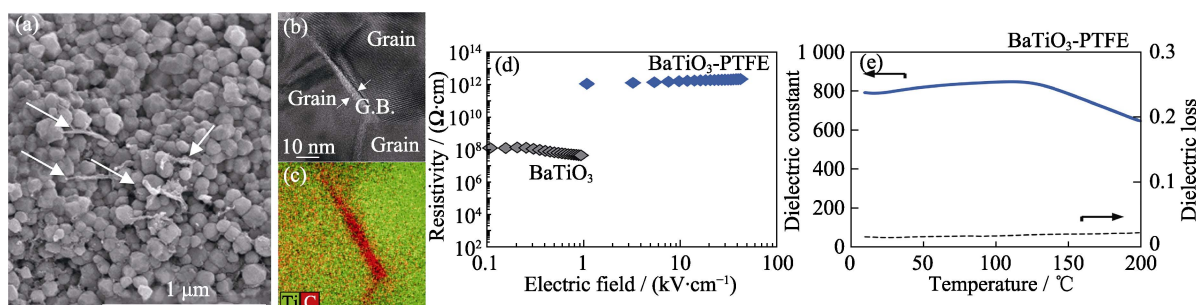


图 10 冷烧结 BaTiO_3 -PTFE 复合材料^[57]

Fig. 10 Cold sintered BaTiO_3 -PTFE composites^[57]

(a) SEM image; (b) TEM image; (c) EDS image; (d) Relationship between resistivity and electric field strength comparing with BaTiO_3 ceramics; (e) Dielectric temperature spectra

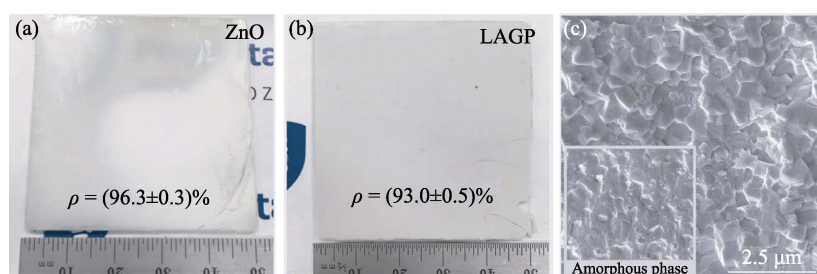
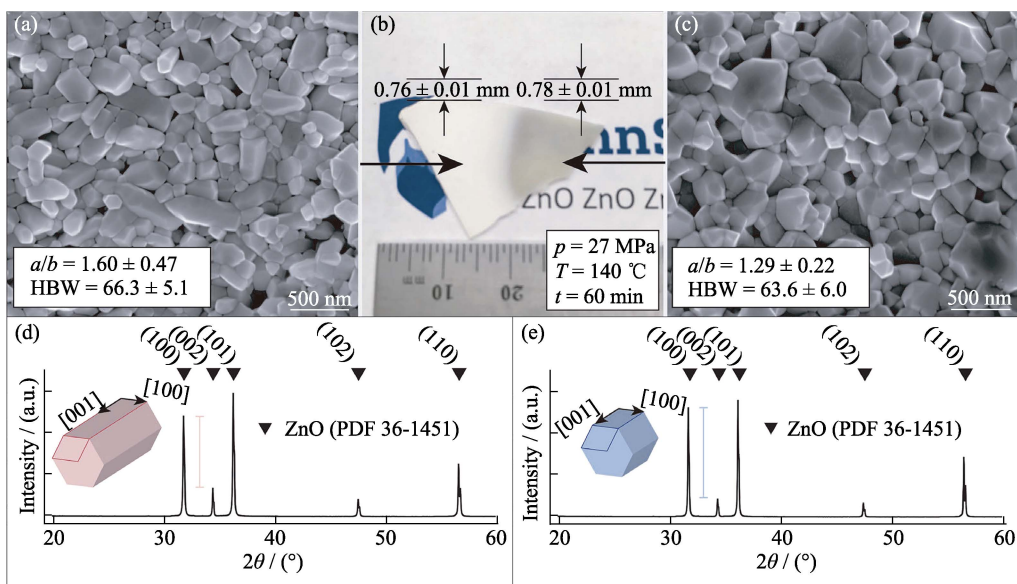


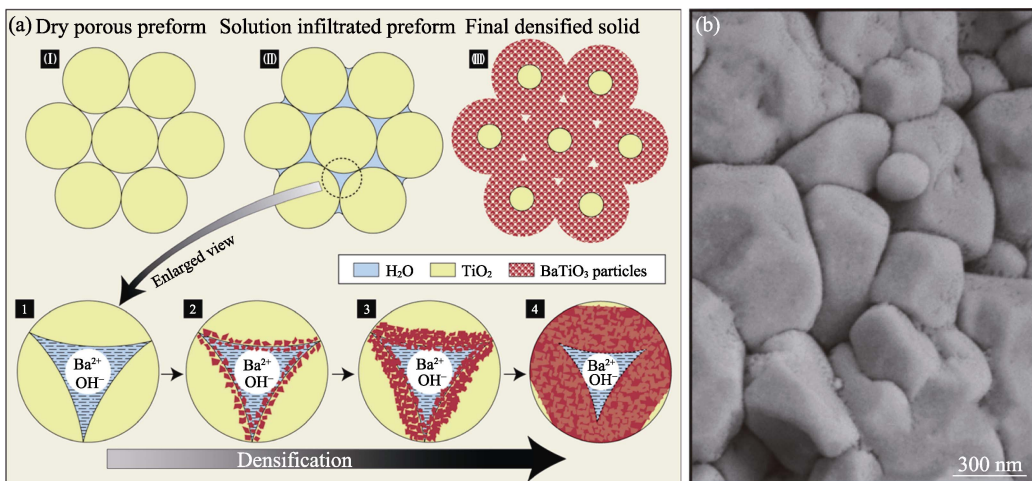
图 11 冷烧结 ZnO 和 LAGP 陶瓷的大尺寸试样^[69]

Fig. 11 Cold sintered ZnO and LAGP ceramic samples with large size^[69]

(a) Photograph of ZnO ; (b) Photograph of LAGP; (c) SEM image of LAGP

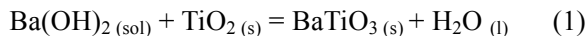
图 12 冷烧结 ZnO 陶瓷的明显不均匀性^[69]Fig. 12 Obvious inhomogeneity of cold sintered ZnO ceramics^[69]

(a) SEM image of opaque area; (b) Photograph; (c) SEM image of translucent area; (d) XRD pattern of opaque area; (e) XRD pattern of translucent area

图 13 反应水热液相致密化技术^[72]Fig. 13 Reactive hydrothermal liquid phase densification process^[72]

(a) Schematic of the HLPD process; (b) SEM image of BaTiO₃/TiO₂ ceramics prepared by rHLPD

生坯，再把 $\text{Ba}(\text{OH})_2 \cdot 8\text{H}_2\text{O}$ 通过水溶液渗透至孔隙结构中，并将该体系置于 240 °C 下进行 72 h 的水热结晶反应，最终获得了致密度约为 90% 的 $\text{BaTiO}_3/\text{TiO}_2$ (其中残留 TiO_2 含量低于 5%) 陶瓷。该技术要求原料体系发生水热结晶反应的同时，反应产物的摩尔体积必须大于生坯，如反应(1)所示， BaTiO_3 ($38.7 \text{ cm}^3/\text{mol}$) 的摩尔体积大于 TiO_2 ($20.2 \text{ cm}^3/\text{mol}$)，才能在水热结晶反应的同时发生摩尔体积膨胀。该过程中孔隙作为局部的微反应器，随着目标反应的摩尔体积膨胀，孔隙空间逐渐被填充从而实现致密化，理论致密度可以达到 91.6%。



该技术在陶瓷致密化过程中无需施加压力，不会导致样品的体积收缩，可以使用多种常规成型技术制备各种形状和尺寸的多孔生坯，而且不存在变形或开裂的风险，比较适合工业化的大规模生产。目前研究者利用该技术已成功实现了 $\text{SrTiO}_3/\text{TiO}_2$ 、 $\text{Ca}(\text{PO}_4)\text{F}_2/\text{CaF}_2$ 、 $\text{Sr}(\text{PO}_4)(\text{OH})_2/\text{SrTiO}_3/\text{TiO}_2$ 、 $\text{CaC}_2\text{O}_4/\text{Ca}(\text{OH})_2$ 、 $\text{CaCO}_3/\text{SiO}_2/\text{CaSiO}_3$ 等陶瓷材料体系的低温烧结^[29,73]。但其无法形成完全纯相的致密化体系，并且对于不同陶瓷体系的适用性还有待进一步探索。但类似于 rHLPD 技术，将化学能引入冷烧结过程，可以大幅提高原子迁移率，通过影响烧结动力学促进传质过程，有效降低冷烧结技术中施加的单

轴压力, 从而实现低温低压烧结, 为解决冷烧结压力过高的问题提供新思路, 为冷烧结技术在工业化大规模生产中的应用指明方向。

4 总结与展望

冷烧结技术是近年来发展起来的一种新的烧结技术, 利用冷烧结技术可以在低于 400 °C 的温度下实现陶瓷材料的快速致密化, 为新材料(尤其是陶瓷-聚合物复合材料)的制备和应用提供了新思路和新机会。冷烧结技术的出现不仅丰富了烧结科学和理论, 也将极大地推动材料科学和技术的发展。尽管冷烧结技术目前已应用于制备近百种陶瓷及复合材料, 但作为一种新技术, 对其烧结机理和各种制备现象的理解还需进一步的研究和探讨。特别是冷烧结致密化需要在较高的压力下进行, 解决烧结压力大的问题, 推动冷烧结技术在新材料和器件生产中的应用将是未来的研究重点。

参考文献:

- [1] VANDIVER P B, SOFFER O, KLIMA B, et al. The origins of ceramic technology at Dolni Věstonice, Czechoslovakia. *Science*, 1989, **246**(4933): 1002.
- [2] GERMAN R M. History of sintering: empirical phase. *Powder Metallurgy*, 2013, **56**(2): 117.
- [3] BORDIA R K, KANG S J L, OLEVSKY E A. Current understanding and future research directions at the onset of the next century of sintering science and technology. *Journal of the American Ceramic Society*, 2017, **100**(6): 2314.
- [4] NDAYISHIMIYE A, SENGUL M Y, BANG S H, et al. Comparing hydrothermal sintering and cold sintering process: mechanisms, microstructure, kinetics and chemistry. *Journal of the European Ceramic Society*, 2020, **40**(4): 1312.
- [5] SMITH B L, SCHÄFFER T E, VIANI M, et al. Molecular mechanistic origin of the toughness of natural adhesives, fibres and composites. *Nature*, 1999, **399**(6738): 761.
- [6] RENARD F, BERNARD D, THIBAULT X, et al. Synchrotron 3D microtomography of halite aggregates during experimental pressure solution creep and evolution of the permeability. *Geophysical Research Letters*, 2004, **31**(7): L07607.
- [7] FU C L, LI X M, GUO J. Recent progress of dielectric materials prepared via cold sintering process. *Journal of Shaanxi Normal University (Natural Science Edition)*, 2021, **49**(4): 30.
- [8] JIANG R Z, LIU J. Research progress of cold sintering technology of ceramics. *Journal of Guiyang University (Natural Science Edition)*, 2021, **16**(4): 60.
- [9] DURAN C, SATO K, HOTTA Y, et al. Eco-friendly processing and methods for ceramic materials: a review. *Journal of the Ceramic Society of Japan*, 2008, **116**(1359): 1175.
- [10] IBN-MOHAMMED T, RANDALL C A, MUSTAPHA K B, et al. Decarbonising ceramic manufacturing: a techno-economic analysis of energy efficient sintering technologies in the functional materials sector. *Journal of the European Ceramic Society*, 2019, **39**(16): 5213.
- [11] TODD R I, ZAPATA-SOLVAS E, BONILLA R S, et al. Electrical characteristics of flash sintering: thermal runaway of Joule heating. *Journal of the European Ceramic Society*, 2015, **35**(6): 1865.
- [12] ZHANG Y, JUNG J I, LUO J. Thermal runaway, flash sintering and asymmetrical microstructural development of ZnO and ZnO-Bi₂O₃ under direct currents. *Acta Materialia*, 2015, **94**: 87.
- [13] BIESUZ M, GRASSO S, SGLAVO V M. What's new in ceramics sintering? A short report on the latest trends and future prospects. *Current Opinion in Solid State & Materials Science*, 2020, **24**(5): 100868.
- [14] GUO J, FLOYD R, LOWUM S, et al. Cold sintering: progress, challenges, and future opportunities. *Annual Review of Materials Research*, 2019, **49**(1): 275.
- [15] COLOGNA M, RASHKOVA B, RAJ R. Flash sintering of nanograin zirconia in <5 s at 850 °C. *Journal of the American Ceramic Society*, 2010, **93**(11): 35569.
- [16] BIESUZ M, SGLAVO V M. Flash sintering of ceramics. *Journal of the European Ceramic Society*, 2019, **39**(2): 115.
- [17] GUO H Z, BAKER A, GUO J, et al. Protocol for ultralow-temperature ceramic sintering: an integration of nanotechnology and the cold sintering process. *ACS Nano*, 2016, **10**(11): 10606.
- [18] GUO H Z, BAKER A, GUO J, et al. Cold sintering process: a novel technique for low-temperature ceramic processing of ferroelectrics. *Journal of the American Ceramic Society*, 2016, **99**(11): 3489.
- [19] GUO J, BERBANO S S, GUO H Z, et al. Cold sintering process of composites: bridging the processing temperature gap of ceramic and polymer materials. *Advanced Functional Materials*, 2016, **26**(39): 7115.
- [20] GUO J, GUO H Z, BAKER A L, et al. Cold sintering: a paradigm shift for processing and integration of ceramics. *Angewandte Chemie International Edition*, 2016, **55**(38): 11457.
- [21] GUO J, BAKER A L, GUO H Z, et al. Cold sintering process: a new era for ceramic packaging and microwave device development. *Journal of the American Ceramic Society*, 2017, **100**(2): 669.
- [22] MUNIR Z A, ANSELMI-TAMBURINI U, OHYANAGI M. The effect of electric field and pressure on the synthesis and consolidation of materials: a review of the spark plasma sintering method. *Journal of Materials Science*, 2006, **41**(3): 763.
- [23] GUILLOU O, GONZALEZ-JULIAN J, DARGATZ B, et al. Field-assisted sintering technology/spark plasma sintering: mechanisms, materials, and technology developments. *Advanced Engineering Materials*, 2014, **16**(7): 830.
- [24] YANAGISAWA K, KANAHARA S, NISHIOKA M, et al. Immobilization of radioactive wastes in hydrothermal synthetic rock, (II). *Journal of Nuclear Science and Technology*, 1984, **21**(7): 558.
- [25] YAMASAKI N, YANAGISAWA K, NISHIOKA M, et al. A hydrothermal hot-pressing method: apparatus and application. *Journal of Materials Science Letters*, 1986, **5**(3): 355.
- [26] YAMASAKI N, KAI T, NISHIOKA M, et al. Porous hydroxyapatite ceramics prepared by hydrothermal hot-pressing. *Journal of Materials Science Letters*, 1990, **9**(10): 1150.
- [27] IOKU K, YAMAMOTO K, YANAGISAWA K, et al. Low temperature sintering of hydroxyapatite by hydrothermal hot-pressing. *Phosphorus Research Bulletin*, 1994, **4**: 65.
- [28] HOSOI K, HASHIDA T, TAKAHASHI H, et al. New processing technique for hydroxyapatite ceramics by the hydrothermal hot-pressing method. *Journal of the American Ceramic Society*, 1996, **79**(10): 2771.
- [29] VAKIFAHMETOGLU C, KARACASULU L. Cold sintering of ceramics and glasses: a review. *Current Opinion in Solid State & Materials Science*, 2020, **24**(1): 100807.
- [30] BOUVILLE F, STUDART A R. Geologically-inspired strong bulk ceramics made with water at room temperature. *Nature Communications*, 2017, **8**(1): 14655.
- [31] INDUJA I J, SEBASTIAN M T. Microwave dielectric properties of mineral sillimanite obtained by conventional and cold sintering process. *Journal of the European Ceramic Society*, 2017, **37**(5): 2143.
- [32] INDUJA I J, SEBASTIAN M T. Microwave dielectric properties of cold sintered Al₂O₃-NaCl composite. *Materials Letters*, 2018, **211**: 55.
- [33] WANG D, ZHOU D, ZHANG S, et al. Cold-sintered temperature stable Na_{0.5}Bi_{0.5}MoO₄-Li₂MoO₄ microwave composite ceramics. *ACS Sustainable Chemistry & Engineering*, 2018, **6**(2): 2438.
- [34] GUO J, ZHAO X T, DE BEAUVOIR T H, et al. Recent progress in applications of the cold sintering process for ceramic-polymer composites. *Advanced Functional Materials*, 2018, **28**(39): 1801724.
- [35] GUO H Z, GUO J, BAKER A, et al. Hydrothermal-assisted cold sintering process: a new guidance for low-temperature ceramic

- sintering. *ACS Applied Materials & Interfaces*, 2016, **8(32)**: 20909.
- [36] HUANG H, TANG J, LIU J. Preparation of $\text{Na}_{0.5}\text{Bi}_{0.5}\text{TiO}_3$ ceramics by hydrothermal-assisted cold sintering. *Ceramics International*, 2019, **45(6)**: 6753.
- [37] YU T, CHENG J, LI L, et al. Current understanding and applications of the cold sintering process. *Frontiers of Chemical Science and Engineering*, 2019, **13(4)**: 654.
- [38] GALLOTTA A, SGLAVO V M. The cold sintering process: a review on processing features, densification mechanisms and perspectives. *Journal of the European Ceramic Society*, 2021, **41(16)**: 1.
- [39] NDAYISHIMIYE A, SENGUL M Y, SADA T, et al. Roadmap for densification in cold sintering: chemical pathways. *Open Ceramics*, 2020, **2**: 100019.
- [40] HONG W B, LI L, CAO M, et al. Plastic deformation and effects of water in room-temperature cold sintering of NaCl microwave dielectric ceramics. *Journal of the American Ceramic Society*, 2018, **101(9)**: 4038.
- [41] HAUG M, BOUVILLE F, RUIZ-AGUDO C, et al. Cold densification and sintering of nanovaterite by pressing with water. *Journal of the European Ceramic Society*, 2020, **40(3)**: 893.
- [42] GONZALEZ-JULIAN J, NEUHAUS K, BERNEMANN M, et al. Unveiling the mechanisms of cold sintering of ZnO at 250 °C by varying applied stress and characterizing grain boundaries by Kelvin Probe Force Microscopy. *Acta Materialia*, 2018, **144**: 116.
- [43] KANG X, FLOYD R, LOWUM S, et al. Cold sintering with dimethyl sulfoxide solutions for metal oxides. *Journal of Materials Science*, 2019, **54(10)**: 7438.
- [44] KANG S, GUO H, WANG J, et al. Influence of surface coating on the microstructures and dielectric properties of BaTiO_3 ceramic via a cold sintering process. *RSC Advances*, 2020, **10**: 30870.
- [45] FAOURI S S, MOSTAED A, DEAN J S, et al. High quality factor cold sintered $\text{Li}_2\text{MoO}_4\text{-BaFe}_{12}\text{O}_{19}$ composites for microwave applications. *Acta Materialia*, 2019, **166**: 202.
- [46] ZHOU D, PANG L X, WANG D W, et al. Novel water-assisting low firing MoO_3 microwave dielectric ceramics. *Journal of the European Ceramic Society*, 2019, **39(7)**: 2374.
- [47] LIU Y, SUN Q, WANG D, et al. Development of the cold sintering process and its application in solid-state lithium batteries. *Journal of Power Sources*, 2018, **393**: 193.
- [48] GUO J, GUO H, HEIDARY D S B, et al. Semiconducting properties of cold sintered V_2O_5 ceramics and Co-sintered $\text{V}_2\text{O}_5\text{-PEDOT:PSS}$ composites. *Journal of the European Ceramic Society*, 2017, **37(4)**: 1529.
- [49] LIU J A, LI C H, SHAN J J, et al. Preparation of high-density InGaZnO_4 target by the assistance of cold sintering. *Materials Science in Semiconductor Processing*, 2018, **84**: 17.
- [50] MARIA J P, KANG X Y, FLOYD R D, et al. Cold sintering: current status and prospects. *Journal of Materials Research*, 2017, **32(17)**: 3205.
- [51] KÄHÄRI H, TEIRIKANGAS M, JUUTI J, et al. Dielectric properties of lithium molybdate ceramic fabricated at room temperature. *Journal of the American Ceramic Society*, 2014, **97(11)**: 3378.
- [52] WU M W, ZHU H F, WANG J F, et al. Review on cold sintering process for preparation of ceramic materials. *China Ceramics*, 2021, **57(3)**: 1.
- [53] KANG S L, ZHAO X T, ZHANG J X, et al. Recent research progress of cold sintering process and its potential application in electrotechnical fields. *Transactions of China Electrotechnical Society*, 2022, **37(5)**: 10984.
- [54] FUNAHASHI S, GUO J, GUO H, et al. Demonstration of the cold sintering process study for the densification and grain growth of ZnO ceramics. *Journal of the American Ceramic Society*, 2017, **100(2)**: 546.
- [55] KANG X, FLOYD R, LOWUM S, et al. Mechanism studies of hydrothermal cold sintering of zinc oxide at near room temperature. *Journal of the American Ceramic Society*, 2019, **102(8)**: 4459.
- [56] TSUJI K, NDAYISHIMIYE A, LOWUM S, et al. Single step densification of high permittivity BaTiO_3 ceramics at 300 °C. *Journal of the European Ceramic Society*, 2020, **40(4)**: 1280.
- [57] SADA T, TSUJI K, NDAYISHIMIYE A, et al. High permittivity BaTiO_3 and $\text{BaTiO}_3\text{-polymer}$ nanocomposites enabled by cold sintering with a new transient chemistry: $\text{Ba}(\text{OH})_2\text{-8H}_2\text{O}$. *Journal of the European Ceramic Society*, 2021, **41(1)**: 409.
- [58] ZHAO Y Y, BERBANO S S, GAO L S, et al. Cold-sintered $\text{V}_2\text{O}_5\text{-PEDOT:PSS}$ nanocomposites for negative temperature coefficient materials. *Journal of the European Ceramic Society*, 2019, **39(4)**: 1257.
- [59] GUO J, PFEIFFENBERGER N, BEESE A, et al. Cold sintering $\text{Na}_2\text{Mo}_2\text{O}_7$ ceramic with poly(ether imide) (PEI) polymer to realize high-performance composites and integrated multilayer circuits. *ACS Applied Nano Materials*, 2018, **1(8)**: 3837.
- [60] NDAYISHIMIYE A, TSUJI K, WANG K, et al. Sintering mechanisms and dielectric properties of cold sintered $(1-x)\text{SiO}_2\text{-}x\text{PTFE}$ composites. *Journal of the European Ceramic Society*, 2019, **39(15)**: 4743.
- [61] SADA T, TSUJI K, NDAYISHIMIYE A, et al. Enhanced high permittivity $\text{BaTiO}_3\text{-polymer}$ nanocomposites from the cold sintering process. *Journal of Applied Physics*, 2020, **128(8)**: 084103.
- [62] ZHAO X T, GUO J, WANG K, et al. Introducing a ZnO-PTFE (polymer) nanocomposite varistor via the cold sintering process. *Advanced Engineering Materials*, 2018, **20(7)**: 1700902.
- [63] SEO J H, GUO J, GUO H Z, et al. Cold sintering of a Li-ion cathode: LiFePO_4 -composite with high volumetric capacity. *Ceramics International*, 2017, **43(17)**: 15370.
- [64] GYAN D S, DWIVEDI A. Structural and electrical characterization of $\text{NaNbO}_3\text{-PVDF}$ nanocomposites fabricated using cold sintering synthesis route. *Journal of Applied Physics*, 2019, **125(2)**: 024103.
- [65] SI M M, GUO J, HAO J Y, et al. Cold sintered composites consisting of PEEK and metal oxides with improved electrical properties via the hybrid interfaces. *Composites Part B-Engineering*, 2021, **226**: 109349.
- [66] SI M M, HAO J Y, ZHAO E D, et al. Preparation of zinc oxide/poly-ether-ether-ketone (PEEK) composites via the cold sintering process. *Acta Materialia*, 2021, **215**: 117036.
- [67] NDAYISHIMIYE A, GRADY Z A, TSUJI K, et al. Thermosetting polymers in cold sintering: the fabrication of $\text{ZnO-polydimethylsiloxane}$ composites. *Journal of the American Ceramic Society*, 2020, **103(5)**: 3039.
- [68] MENA-GARCIA J, DURSUN S, TSUJI K, et al. Integration and characterization of a ferroelectric polymer PVDF-TrFE into the grain boundary structure of ZnO via cold sintering. *Journal of the European Ceramic Society*, 2022, **42(6)**: 2789.
- [69] BANG S H, TSUJI K, NDAYISHIMIYE A, et al. Toward a size scale-up cold sintering process at reduced uniaxial pressure. *Journal of the American Ceramic Society*, 2020, **103(4)**: 2322.
- [70] SEO J H, NAKAYA H, TAKEUCHI Y, et al. Broad temperature dependence, high conductivity, and structure-property relations of cold sintering of LLZO-based composite electrolytes. *Journal of the European Ceramic Society*, 2020, **40(15)**: 6241.
- [71] DE BEAUVOIR T H, TSUJI K, ZHAO X, et al. Cold sintering of ZnO-PTFE : utilizing polymer phase to promote ceramic anisotropic grain growth. *Acta Materialia*, 2020, **186**: 511.
- [72] VAKIFAHMETOGLU C, ANGER J F, ATAKAN V, et al. Reactive hydrothermal liquid-phase densification (rHLPD) of ceramics: a study of the $\text{BaTiO}_3\text{-}[\text{TiO}_2]$ composite system. *Journal of the American Ceramic Society*, 2016, **99(12)**: 3893.
- [73] LI Q, GUPTA S, TANG L, et al. A novel strategy for carbon capture and sequestration by rHLPD processing. *Frontiers in Energy Research*, 2016, **3**: 53.